Voltage-activated Currents in Guinea Pig Pancreatic α_2 Cells

Evidence for Ca^{2+}-dependent Action Potentials

P. RORSMAN and B. HELLMAN

From the Department of Medical Cell Biology, Biomedicum, S-751 23 Uppsala, Sweden

ABSTRACT Glucagon-secreting α_2 cells were isolated from guinea pig pancreatic islets and used for electrophysiological studies of voltage-activated ionic conductances using the patch-clamp technique. The α_2 cells differed from β cells in producing action potentials in the absence of glucose. The frequency of these potentials increased after addition of 10 mM arginine but remained unaffected in the presence of 5–20 mM glucose. When studying the conductances underlying the action potentials, we identified a delayed rectifying K^+ current, an Na^+ current, and a Ca^{2+} current. The K^+ current activated above −20 mV and then increased with the applied voltage. The Na^+ current developed at potentials above −50 mV and reached a maximal peak amplitude of 550 pA during depolarizing pulses to −15 mV. The Na^+ current inactivated rapidly ($\tau_h \sim 0.7$ ms at 0 mV). Half-maximal steady state inactivation was attained at −58 mV, and currents could no longer be elicited after conditioning pulses to potentials above −40 mV. The Ca^{2+} current first became detectable at −50 mV and reached a maximal amplitude of 90 pA (in extracellular $[Ca^{2+}] = 2.6$ mM) at about −10 mV. Unlike the Na^+ current, it inactivated little or not at all. Membrane potential measurements demonstrated that both the Ca^{2+} and Na^+ currents contribute to the generation of the action potential. Whereas there was an absolute requirement of extracellular Ca^{2+} for action potentials to be elicited at all, suppression of the much larger Na^+ current only reduced the upstroke velocity of the spikes. It is suggested that this behavior reflects the participation of a low-threshold Ca^{2+} conductance in the pacemaking of α_2 cells.

INTRODUCTION

The mechanisms for stimulus-secretion coupling in the glucagon-producing α_2 cells in the islets of Langerhans are unclear. A key role has been postulated for Ca^{2+} in this process. However, there is disagreement about whether removal of extracellular Ca^{2+} stimulates or inhibits the release of glucagon (LeClercq-Meyer

Address reprint requests to Dr. P. Rorsman, Dept. of Medical Biophysics, Gothenburg University, Box 33031, S-400 33, Göteborg, Sweden.

J. GEN. PHYSIOL. © The Rockefeller University Press · 0022-1295/88/02/0223/20 $2.00

Volume 91 February 1988 223–242

and Malaisse, 1983). Like the insulin-producing β cells, α_2 cells have been shown to generate Ca^{2+}-dependent action potentials (Ikeuchi and Yagi, 1982). Evidence has been produced for electrical coupling between α_2 and β cells mediated by gap junctions (Orci et al., 1976; Michaels and Sheridan, 1981; Meda et al., 1982). These observations have led to the belief that glucose induces an electrical activity in α_2 cells similar to that observed in β cells (Meda et al., 1986). The latter proposal is somewhat surprising, since glucose has opposite effects on the secretion from the two types of cells.

In the present investigation, the patch-clamp technique (Hamill et al., 1981) was used for electrophysiological studies on α_2 cells, with particular emphasis on their voltage-activated currents. It will be shown that these cells differ from β cells in producing action potentials in the absence of glucose. In demonstrating that exposure of α_2 cells to the powerful secretagogue arginine results in an increased frequency of action potentials and that these are, at least in part, attributable to an inward Ca^{2+} current, the present study supports the notion that glucagon secretion is a process dependent on influx of Ca^{2+}.

METHODS

Solutions

The compositions of the different extracellular and intracellular media used in this and the accompanying article (Rorsman, 1988) are given in Table I. In the whole-cell configuration of the patch-clamp technique, the pipette solution diffuses into the intracellular space. It should consequently have a composition that mimics that of the cytoplasm (high K^+ and low Ca^{2+}). For the study of inward currents, it was necessary to block outward K^+ currents. This was achieved by substituting the membrane-impermeant cation *N*-methyl-D-glucamine$^+$ (NMDG; positively charged at physiological pH) for the K^+ in the pipette (compare solutions E and F). ATP (3 mM) was usually included in the intracellular media. This additive was necessary to prevent the development of an ATP-regulated K^+ conductance in β cells (Cook and Hales, 1984; Rorsman and Trube, 1985). No such conductance was observed in α_2 cells. However, ATP was also included in the intracellular media when the latter cells were studied, since it has been found to improve Ca^{2+} channel maintenance in other cells (Fedulova et al., 1985; Byerly and Yazejian, 1986). The basal extracellular medium was a HEPES-buffered solution balanced in cations with Cl^- as the sole anion. When Ca^{2+} currents were studied, the Na^+ current was blocked either by omission of extracellular Na^+ or by inclusion of the Na^+ channel blocker tetrodotoxin (TTX). Na^+ currents could be separated from the Ca^{2+} currents after exclusion of extracellular Ca^{2+} and addition of the inorganic Ca^{2+} channel blocker Co^{2+}. The bath used in the electrophysiological experiments had a volume of 1.5 ml and could be perfused at a rate of 4–5 ml/min. As indicated by the disappearance of the Na^+ current when perfusing with a medium in which Na^+ was replaced by choline, exchange of the solution in the bath was complete within 1 min.

Electrophysiology

The cell-attached patch configuration and the whole-cell recording mode of the patch-clamp technique were employed (Hamill et al., 1981; Fenwick et al., 1982*a*). Pipettes were pulled from aluminosilicate glass (Hilgenberg, Malsfeld, Federal Republic of Germany [FRG]) and coated with silicone rubber (RTV615A, General Electric, Waterford, NY). The pipette was connected to a patch-clamp amplifier (EPC-7, List-Electronic,

Darmstadt, FRG), allowing compensation of capacitance and series resistance. After being filled with isotonic saline or high K^+, the pipettes had resistances between 3 and 5 MΩ. The resistance was slightly higher when NMDG was used. A tight seal (>10 GΩ) was established between the cell membrane and the tip of the pipette by gentle suction. Seal formation was facilitated by applying a negative potential (−80 mV) to the pipette. Pipette resistances increased to 5–50 MΩ when the patch membrane was disrupted to establish the whole-cell configuration. Using the series resistance compensation of the amplifier, the voltage error during current flow was kept to <10 mV and in most experiments amounted to only ~1 mV. The pulse programs for the voltage-clamp and current-injection experiments were produced by a programmable stimulator (PGW, Stühmer Elektronik, Göttingen, FRG). Membrane potentials could be recorded by switching the amplifier to the current-clamp mode. All experiments were performed at room temperature (20–25°C).

TABLE I

Composition of Media

	Extracellular					Intracellular	
	A	B	C	D		E	F
	mM					*mM*	
NaCl	138	138	69	—	KCl	125	—
KCl	5.6	5.6	5.6	5.6	NMDG	—	150
$MgCl_2$	1.2	1.2	1.2	1.2	$MgCl_2$	4	1
$CaCl_2$	2.6/10.2	—	—	2.6/10.2	$CaCl_2$	2	2
HEPES (NaOH)	10	10	10	10	EGTA	10	10
Choline-Cl	—	—	69	138	HCl	—	110
$CoCl_2$	—	2	2	(5)	KOH	30	—
TTX (*μg/ml*)	(2.5)	—	—	—	HEPES	5	5
D-600 (*μM*)	—	—	—	(25)	Na_2ATP	3	3
Nifedipine (*μM*)	—	—	—	(15)	pH	7.15	7.15
pH	7.4	7.4	7.4	7.4		(KOH)	(HCl)

Compositions of the different extracellular (A–D) and intracellular (E and F) media are given. In the extracellular media, the pH was adjusted to 7.4 with NaOH; in the intracellular media, it was adjusted to 7.15 using HCl or KOH. The values in parentheses indicate that the compound was not usually present, but was added at the concentration given when included. Two concentrations of Ca^{2+} were used: 2.6 and 10.2 mM. D-600, nifedipine, and forskolin were added as concentrated stock solutions in DMSO (dimethylsulfoxide; final concentration, 0.1%). In the intracellular media, the free concentrations of Ca^{2+} and Mg^{2+} were calculated as 0.06 μM and 1.2 mM, respectively, from the binding constants of Martell and Smith (1974).

Data Analysis

During the experiments, the current and voltage signals were recorded on videotape by a digital audio processor and a modified (Bezanilla, 1985) video cassette recorder (SL 2000, Sony Corp., Tokyo, Japan). The current signal was filtered at 1–4 kHz (−3 dB) by a four-pole Bessel low-pass filter (AF 173, Lötscher Elektronik, Andelfingen, FRG). The data were evaluated on a digital oscilloscope (3091, Nicolet Instrument Corp., Madison, WI). Current amplitudes were measured directly from the oscilloscope, and the time courses for the development and inactivation of the currents were approximated to exponential functions after plotting on an *X-Y* recorder. Current-voltage (*I-V*) relationships were compensated for linear leakage. This was estimated by extrapolation from a straight line constructed by linear regression for the current-voltage relationship, obtained by applying small voltage pulses around the holding potential. The input resistance of the

cell was determined accordingly, and values for the cell capacitance were measured directly from the amplifier.

Preparation and Identification of α_2 Cells

Islets of Langerhans were isolated, by collagenase digestion, from the splenic part of the pancreases (to avoid contamination with pancreatic polypeptide-containing cells) of pigmented 2–4-mo-old guinea pigs. The islets were dissociated into single cells by vigorous shaking in a Ca^{2+}-free medium containing no enzymes (Lernmark, 1974). The cell suspension was plated on petri dishes and maintained in culture for up to a week in RPMI 1640 medium containing 5.5 mM glucose and supplemented with 10% vol/vol heat-inactivated fetal calf serum, 100 U/ml penicillin, 100 μg/ml streptomycin, and 60 μg/ml gentamycin.

Patch-clamp studies on a 75–85% pure α_2 cell fraction, obtained by autofluorescence-activated cell sorting (Pipeleers et al., 1985), demonstrated that rat α_2 cells differ from β cells in producing action potentials in the absence of glucose (Wesslén et al., 1987). As shown in previous studies, the glucagon-secreting α_2 cells can easily be identified in guinea pigs on the basis of their large size and bright appearance under the dark-field microscope (Petersson et al., 1962; Petersson, 1966; Brolin et al., 1966; Lundquist et al., 1970). Immunohistochemistry performed on the tissue-cultured islet cells not only confirmed that the large cells (20–25 μm diam) were α_2 cells, but also revealed that the somatostatin-secreting α_1 cells differed from the other islet cells in being restricted to the clusters (Grimelius, L., and G. Hacker, personal communication). Thus, by choosing single and large cells producing action potentials in the absence of glucose, the α_2 cells could be conveniently and safely identified. In early experiments, we also checked that such cells appeared bright under the dark-field microscope but this step was later left out.

RESULTS

Comparison of Currents in β Cells from Guinea Pigs with Those in Other Species

For comparative purposes, we first ascertained that β cells from guinea pigs have electrophysiological characteristics similar to those of the rat and mouse. Fig. 1 *A* shows examples of channel openings observed at different pipette potentials, when recording from a cell-attached patch in the absence of glucose. It can be seen that the openings of the channel are grouped in bursts and that there are numerous openings and closures of the channel within each burst. Fig. 1 *B* shows that the *I-V* relationship recorded with pipettes containing high K^+ is linear at pipette potentials below 30 mV. The slope corresponds to a single-channel conductance of 62 ± 2 pS ($n = 4$), and the curve can be extrapolated to a reversal at 70 ± 3 mV ($n = 4$), as expected for a K^+ channel in a cell with a membrane potential of −60 to −70 mV and an intracellular K^+ concentration of 120 mM (Meissner et al., 1978).

When 20 mM glucose was added to the bath, channel activity ceased within a few minutes and the cell started producing biphasic spikes that we interpreted as action potentials (cf. Rorsman and Trube, 1985, 1986). After removal from the bath, the effects of glucose were reversed, with a similar time course (not shown). Hence, the general appearance of the channel openings, single-channel conductance, reversal potential, and influence of glucose conform with what is known about the ATP-regulated K^+ channel in β cells from other species (Ashcroft et

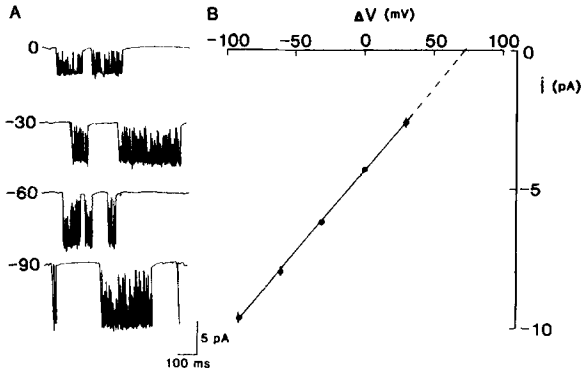

FIGURE 1. Single-channel currents from a cell-attached patch on a β cell. (*A*) The numbers to the left of each trace indicate the shift in patch potential (ΔV) with respect to the cell's resting potential (V_r). For example, −30 mV indicates a patch potential 30 mV more negative than V_r. (*B*) The current amplitudes of channels plotted against the respective potentials (ΔV). Curves were fitted to the individual experimental data by least-squares regression analysis, yielding values for the single-channel conductance (γ) of 62 ± 2 pS and for the reversal potential of 70 ± 3 mV. The curve was drawn by eye. The pipette was filled with medium E and the bath with extracellular medium A containing 2.6 mM Ca^{2+}. Mean values ± SEM are given for four separate patches.

al., 1984; Cook and Hales, 1984; Findlay et al., 1985; Rorsman and Trube, 1985). Subsequently, we tested whether guinea pig β cells possess voltage-activated currents similar to those of mouse β cells (Rorsman and Trube, 1986). This was the case. Fig. 2, *A* and *B*, shows the inward membrane currents obtained when the β cells were subjected to depolarizing voltage pulses from a holding potential of −70 mV. Current responses below −50 mV were negligible, but pulses to more positive potentials evoked clear inward currents, reaching their maxima within 10 ms. The amplitudes of these currents increased when the

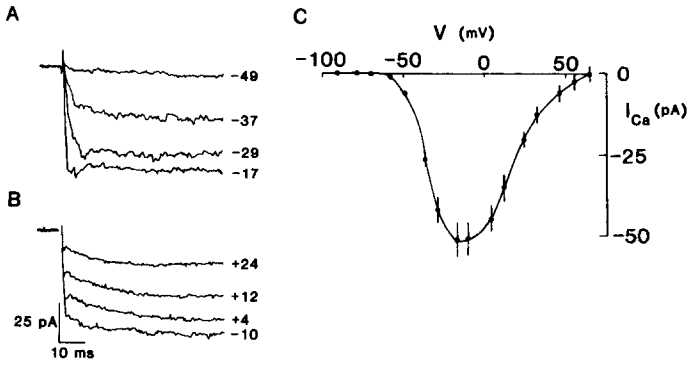

FIGURE 2. Inward Ca^{2+} currents in a β cell. (*A* and *B*) Inward membrane currents were recorded when intracellular K^+ was replaced by NMDG (medium F) and the bath was filled with medium A containing 2.6 mM Ca^{2+}. The holding potential was −70 mV, and the test potentials are indicated to the right of the traces. The pulse duration was 50 ms, with a frequency of 0.5 Hz. (*C*) *I-V* relationship of the peak currents. Mean values ± SEM for 10 experiments.

extracellular Ca^{2+} concentration was raised from 2.6 to 10.2 mM (not shown), which indicates their dependence on extracellular Ca^{2+}. The currents inactivated only slightly, or not at all, during 50-ms pulses. Fig. 2*C* shows the resulting *I-V* relationship. The current reached a maximum at −20 mV, amounting to 50 pA with 2.6 mM Ca^{2+}. At more positive potentials, the size of the current subsequently declined because of the decreased driving force, with a reversal at ~60 mV.

In some cells (~40%), there was an indication of a spiky component at potentials above zero. This component differed from the slow Ca^{2+} current in developing and inactivating rapidly (not shown). Since this component was suppressed by TTX, it probably reflects the opening of voltage-dependent Na^+ channels. Therefore, it seems likely that β cells possess an Na^+ current that is either small

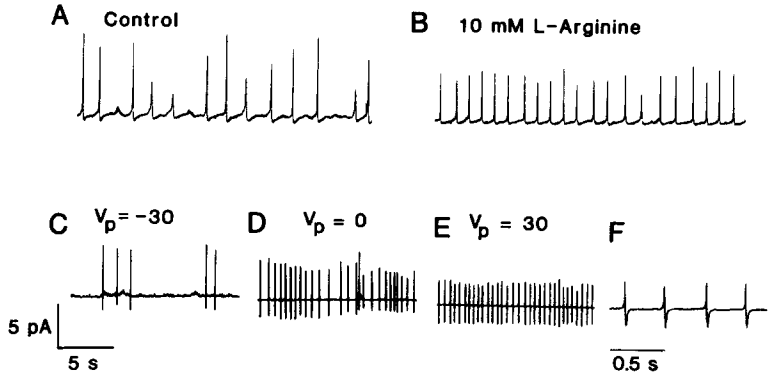

FIGURE 3. Electrical activity of an α_2 cell recorded extracellularly. (*A*) Biphasic current deflections (action potentials) observed under basal condition (absence of glucose). (*B*) After addition of 10 mM L-arginine. Note the increased spike frequency. (*C–F*) Influence of membrane potential on spike frequency. (*C*) Current deflections after applying a negative potential (−30 mV) to the patch. (*D*) Current deflections at cell's membrane potential. (*E*) Action currents after applying a positive potential (30 mV) to the patch. (*F*) Expanded section of trace *E* to demonstrate the biphasic appearance. Note the reduction and increase of spike frequency in traces *C* and *E* relative to that in *D*. The pipette and bath contained normal extracellular medium A with 2.6 mM Ca^{2+}.

or already partially inactivated at −70 mV (Satin and Cook, 1986; Rorsman, 1986). However, in many cells it is obscured by a larger Ca^{2+} current. It was evident from other experiments (not shown) that guinea pig β cells also possess an outward delayed rectifying K^+ current similar to that described in mouse β cells (Rorsman and Trube, 1986). The above-mentioned findings indicate that β cells isolated from guinea pigs display the same current pattern as those from other rodents.

Extracellular Action Potential Recordings from α_2 Cells

Fig. 3 shows the electrical activity of an α_2 cell recorded from a cell-attached patch. The α_2 cell produced action potentials under basal conditions (Fig. 3*A*). The frequency of the action potentials remained unaffected after addition of

5–20 mM glucose (not shown), but increased in the presence of 10 mM arginine (Fig. 3*B*). Fig. 3, *C–E*, shows that the spike frequency is modulated by the membrane potential. Depolarizing the patch, which hyperpolarizes the cell (Fischmeister et al., 1986), reduced the spike frequency (*C*), whereas hyperpolarization of the patch (depolarization of cell) increased the spike frequency (*E*) relative to that observed when no potential was applied to the patch (*D*). Fig. 3*F* shows expanded examples of the biphasic action currents, reflecting the action

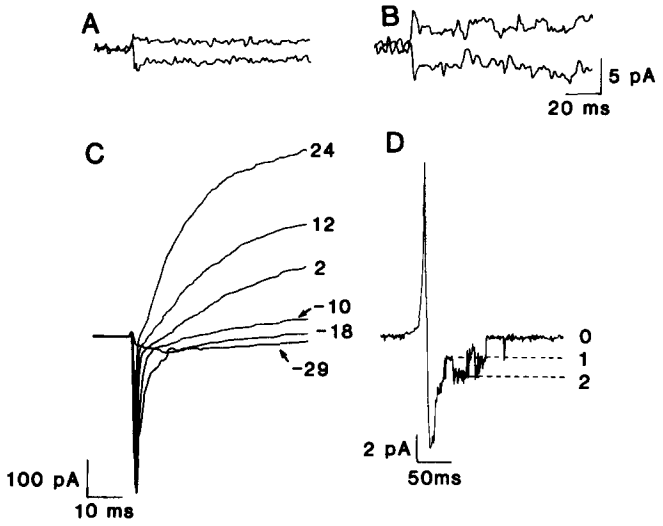

FIGURE 4. Outward and inward currents in α_2 cells. (*A* and *B*) The cell was clamped at −70 mV, and small voltage pulses going to −59 and −79 mV were applied to visualize conductance changes around the holding potential. The records in *A* were obtained immediately after establishing the whole-cell configuration and the records in *B* were obtained after 10 min of intracellular dialysis with the pipette medium. No major change occurred. The records in *B* appear more noisy, because the RS compensation was switched on. (*C*) Whole-cell currents after application of depolarizing pulses to the indicated potentials from −70 mV. The pulses activate inward and outward currents. (*D*) Extracellular action potential from a cell-attached patch recorded before forming the whole-cell mode. The action potential activates K^+ channels (inward because of high K^+ in the pipette) within the patch. Current levels corresponding to zero, one, and two simultaneous openings are indicated. The bath was filled with normal extracellular medium A and the pipettes contained intracellular medium E without ATP. In panels *A–C*, the pulses were 50 ms long and were applied at a rate of 0.5 Hz.

potentials seen via the resistive-capacitative network of the patch, as described by Fenwick et al. (1982*a*).

K^+ Conductances of α_2 Cells

Pancreatic β cells, including those of guinea pigs (Fig. 1), are known to contain a K^+ conductance regulated by intracellular ATP (Cook and Hales, 1984; Findlay et al., 1985; Rorsman and Trube, 1985). To test whether this channel is also

present in the α_2 cell membrane, we performed whole-cell experiments with pipettes filled with an intracellular solution lacking ATP. Fig. 4*A* shows the current responses obtained when small voltage pulses (about ±10 mV) were applied from the holding potential (−70 mV) immediately after establishment of the whole-cell configuration. The voltage pulses result in only minute currents, which indicated a high input resistance of the cell (6 GΩ). Despite the absence of intracellular ATP, the input resistance decreased only slightly over 10 min (4 GΩ; Fig. 4*B*). The small increase of the current responses probably reflects a general deterioration of the seal. This stability is in direct contrast to the dramatic increase of the input conductance that rapidly developed when the guinea pig β

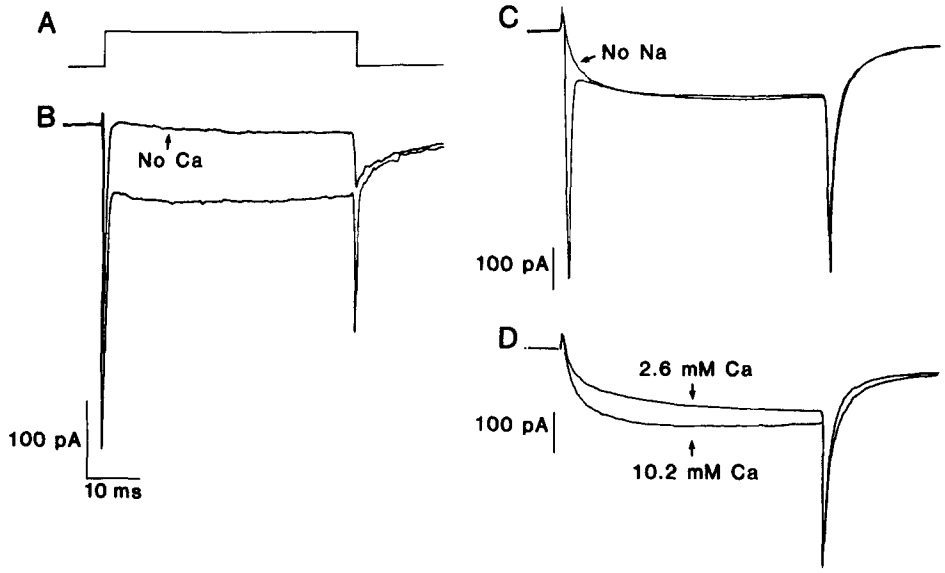

FIGURE 5. Crude identification of α_2 cell inward membrane currents. (*A*) Schematic pulse program. The cell was held at −70 mV. Pulses (50 ms long) going to zero were applied at a rate of 0.5 Hz. (*B*) Effect of removing extracellular Ca^{2+} (medium A replaced by B). Note the disappearance of the sustained component and reduction of the tail current. (*C*) Effect of removal of extracellular Na^+ (medium A replaced by D). Only the fast spiky part was affected. (*D*) Effect of increasing Ca^{2+} from 2.6 to 10.2 mM in the absence of Na^+. Note the increase in current size. The pipettes were filled with intracellular medium F.

cell was dialyzed with the ATP-free solution (not shown, but see Rorsman and Trube, 1985). Fig. 4*C* shows the inward and outward currents obtained when larger voltages were applied. Whereas an inward current first became detectable at −50 mV, a pulse to −20 mV was necessary for the detection of the outward current. The outward current grew with increasing stimuli. It is possible that the outward current reflects the development of a delayed rectifying K^+ current, similar to that in axons (Hodgkin and Huxley, 1952*a*), but the participation of other K^+ conductances, such as Ca^{2+}-activated K^+ channels, cannot be excluded. However, as illustrated in Fig. 4*D*, the K^+ channel that activates during the

action potential is relatively small. At the end of the action potential, when the cell's membrane potential is about −70 mV, this channel has an amplitude of only 1.5 pA, i.e., much smaller than the large Ca^{2+}-activated channel, which at this voltage has an amplitude of ~10 pA (not shown).

Crude Identification of Inward Currents Underlying the α_2 Cell Action Potential

A crude identification of the voltage-activated inward conductances that produce the action potentials is given in Fig. 5. The α_2 cells, known to generate action potentials in the absence of glucose in the cell-attached configuration, were clamped at −70 mV after the whole-cell configuration was established. The intracellular solution lacked K^+ to block the outward K^+ conductance, which would otherwise obscure the inward currents. When the cells were immersed in normal extracellular medium (140 mM Na^+ and 2.6 mM Ca^{2+}), a depolarizing voltage-clamp step to 0 mV produced an inward current consisting of a fast spiky and a sustained component (Fig. 5*B*). The sustained current disappeared after

TABLE II

Electrical Properties of Pancreatic β and α_2 Cells

Type	C_c	R_c	I_{Na}	I_{Ca}
	pF	*GΩ*	*pA/pF*	*pA/pF*
β cells	4.3±0.3	10.9±1.5	—	12.4±1.8
	(17)	(16)		(10)
α_2 cells	11.8±0.4	9.9±0.9	54.5±8.9	9.2±1.2
	(78)	(46)	(12)	(11)

Cell capacitance (C_c), input resistance (R_c), peak Na^+ current (I_{Na}), and peak Ca^{2+} current (I_{Ca}) are given. Values of peak currents are expressed in picoamperes per picofaraday to compensate for variations in size. All values are means ± SEM for the indicated number of experiments. Only β cells without Na^+ currents are included in this table. Ca^{2+} currents were studied from a holding potential of −70 mV and Na^+ currents were studied from a holding potential of −100 mV.

replacement of extracellular Ca^{2+} by Co^{2+} (Fig. 5*B*, top trace) and increased in size after increasing extracellular Ca^{2+} from 2.6 to 10.2 mM (Fig. 5*D*), which suggests that it is carried by Ca^{2+}. Since the transient spiky portion disappeared in the absence of extracellular Na^+ (Fig. 5*C*) and in the presence of the Na^+ channel blocker TTX (not shown), it was attributed to an Na^+ current. From the results shown in Fig. 5, it can be concluded that pancreatic α_2 cells possess voltage-activated inward conductances for both Na^+ and Ca^{2+}.

Comparisons of Current Densities in β and α_2 Cells

Table II summarizes some electrical characteristics of pancreatic α_2 and β cells. The larger size of α_2 cells is reflected by a threefold-higher cell capacitance. In both cell types, the input resistances averaged ~10 GΩ, with values occasionally as high as 25 GΩ. The higher values can be assumed to represent more accurate estimates of the true input resistance, since the lower values probably result from a larger leak conductance. When measured with NMDG-filled pipettes, the specific membrane resistances (normalized by cell capacitance) in the β and α_2

cells were 45.0 ± 5.9 kΩ·μF (n = 16) and 115.0 ± 9.5 kΩ·μF (n = 47; $P <$ 0.001), respectively. Again, the true values can be assumed to be higher because of the influence of leak. The Na^+ current of the α_2 cells corresponds to a density of 50 $\mu A/cm^2$ (assuming a conversion factor of 1 $\mu F/cm^2$). This figure is of the same order of magnitude as the Na^+ current in chromaffin cells (Fenwick et al., 1982*b*) and rat insulinoma cells (Rorsman et al., 1986). The α_2 cells had a slightly lower (25%) Ca^{2+} current than the β cells, when allowance was made for the differences in cell size.

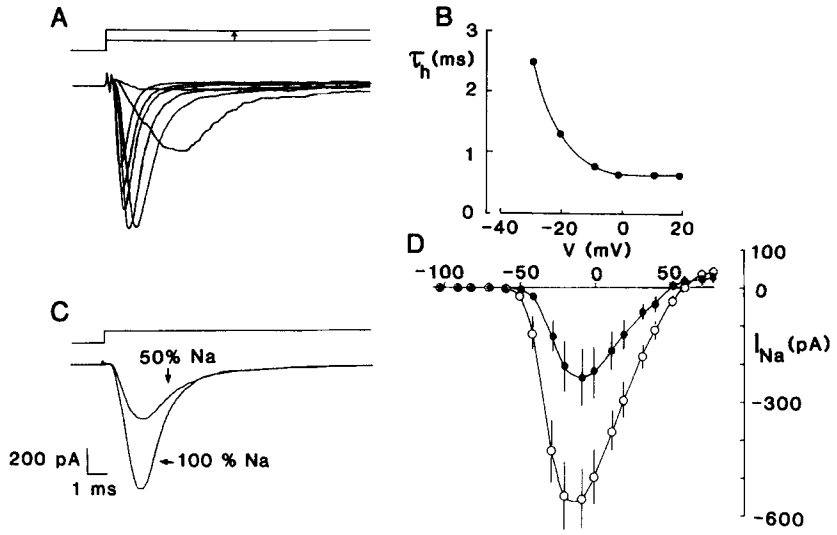

FIGURE 6. Na^+ currents in α_2 cells. (*A*) The cells were clamped at −100 mV and depolarizing pulses (50 ms long) going to potentials between −100 and +80 mV were applied at a rate of 0.5 Hz. The inward Na^+ currents evoked by voltage pulses to −43, −30, −22, −10, −1, 11, and 19 mV are shown. Peak current amplitudes are indicated by dashes to the right of the respective membrane potential values. (*B*) Effects of voltage on time constant of inactivation (τ_h). Values were obtained from an experiment similar to that shown in *A* approximating the observed currents' time courses to Eq. 1. (*C*) Same as panel *A* but with a pulse going to −30 mV. After extracellular Na^+ was lowered to 50%, the current amplitude was correspondingly reduced. (*D*) *I-V* relationship for normal (○) and low (●) extracellular Na^+. Mean values ± SEM of 6 (●) and 13 (○) experiments. Pipettes were filled with intracellular medium F and the bath contained medium B or C.

Voltage Dependence of Na^+ Currents

The Na^+ currents of α_2 cells were studied after suppression of the outward K^+ and inward Ca^{2+} conductances. Fig. 6*A* shows a representative family of voltage-clamp currents obtained when depolarizing pulses were applied from a holding potential of −100 mV. It is evident that the Na^+ currents of the α_2 cells resemble those observed in other types of tissues (Hille, 1984). With increasing depolarizing commands, the turn-on of the Na^+ current becomes progressively faster, reaching a maximum at potentials above −10 mV. The Na^+ currents also

inactivated rapidly. The amplitude of the current size during inactivation could be fitted (neglecting some initial deviation) to the exponential

$$I(t) = I_{max} \cdot e^{-(t/\tau_h)}, \quad (1)$$

where I is the current, t is the time after the beginning of the pulse, I_{max} is the starting value obtained by extrapolating the time course during inactivation to time 0, and τ_h is the time constant of inactivation. The time constant of inactivation decreased from a value of ~2.5 ms at −30 mV to 0.7 ms during stimuli to ≥0 mV (Fig. 6*B*).

Fig. 6*C* demonstrates the dependence of the current on extracellular Na^+. Replacing 50% of the extracellular Na^+ with $choline^+$ resulted in a corresponding reduction of the current. The *I-V* relationships for the two Na^+ concentrations

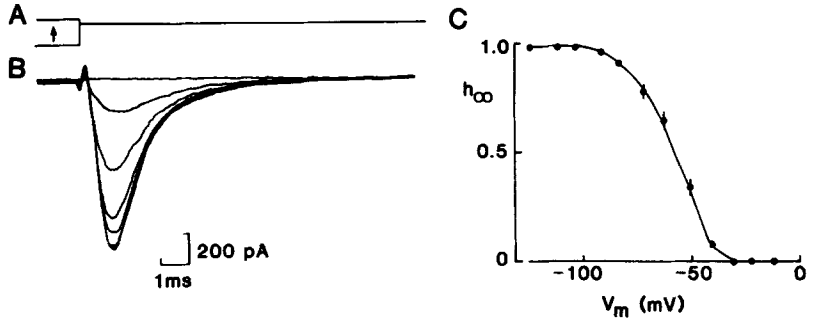

FIGURE 7. Steady state inactivation of Na^+ currents in pancreatic α_2 cells. (*A*) Schematic pulse program. Conditioning pulses (50 ms) were applied between −130 and 0 mV before giving a 50-ms standard pulse to −22 mV. The pulse frequency was 0.5 Hz. (*B*) Na^+ currents observed during a voltage-clamp step to −22 mV after conditioning prepulses going to (from bottom to top) −125, −90, −82, −72, −62, −52, and −40 mV. (*C*) Inactivation curve of Na^+ currents. The relative peak amplitude (h_∞) seen during the conditioning pulse (V_m). The current size obtained subsequent to a conditioning pulse to −132 mV was taken as unity. Data are presented as mean values ± SEM for 12 separate experiments. The pipettes contained medium F and the bath was filled with medium B.

are shown in Fig. 6*D*. It can be seen that the voltage dependence is very steep, and that the maxima for the two curves lie between −20 and −10 mV. The peak amplitude at normal extracellular Na^+ was quite variable from cell to cell and ranged between 200 pA and 1.4 nA in cells of approximately the same size. At positive potentials, the current sizes decrease (reflecting diminished driving force), and the curves intersect the abscissa at 50 and 60 mV for the low and high Na^+ concentrations, respectively. Although these values are lower than those expected from the Nernst equation (80 and 65 mV for extracellular Na^+ concentrations of 143 and 74 mM), there is little doubt that the current is carried primarily by Na^+. This conclusion is reinforced by the observed results of adding TTX and replacing Na^+ with $choline^+$.

Inactivation of Na^+ Currents

To study the voltage dependence of the steady state inactivation of the Na^+ current, α_2 cells were subjected to a standard two-pulse protocol (Hodgkin and Huxley, 1952*b*). Fig. 7*B* shows the currents recorded during a standard test pulse to −20 mV. It can be observed that the current size remained virtually unchanged when the conditioning pulses went to membrane potentials more negative than −90 mV. At more positive voltages, the current size rapidly decreased, and after a prepulse to −40 mV, inactivation was almost complete (Fig. 7*C*). The relationship between the membrane potential during the conditioning pulse (V_m) and the ratio between the observed peak current and the

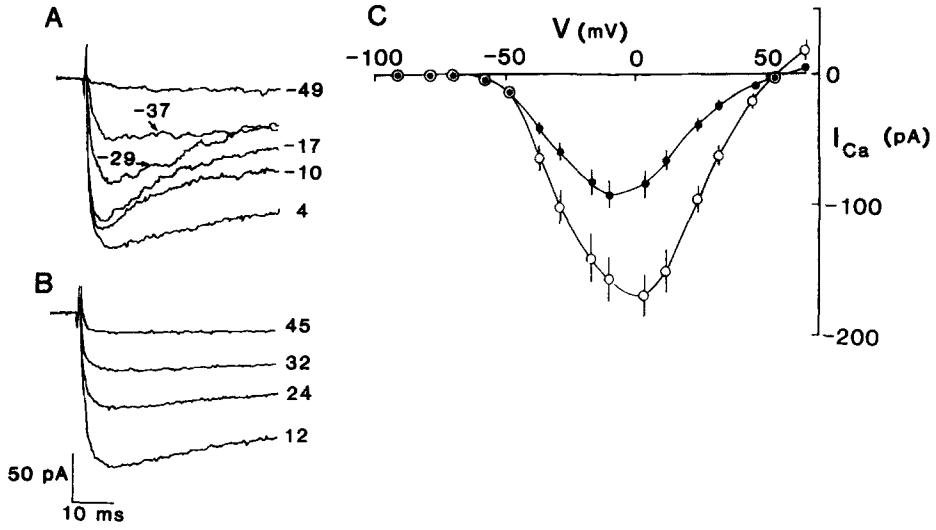

FIGURE 8. Ca^{2+} currents in α_2 cells. (*A* and *B*) Inward Ca^{2+} current observed after depolarizing the cell to indicated potentials from a holding potential of −70 mV. The pulse duration was 50 ms, with a frequency of 0.5 Hz. The pipette contained intracellular medium F and the bath was filled with extracellular medium D with 10.2 mM Ca^{2+}. (*C*) *I-V* relationship of the peak inward current observed with 2.6 (●) or 10.2 (○) mM Ca^{2+}. Na^+ currents were suppressed either by omission of Na^+ (replacement with choline$^+$) or introduction of TTX (2.5 μg/ml). Mean values ± SEM for 17–20 experiments.

maximal response ($I/I_{max} = h_\infty$) was approximated by the Hodgkin-Huxley equation:

$$h_\infty(V_m) = 1/\{1 + \exp[(V_h - V_m)/k_h]\}, \quad (2)$$

where V_h is the membrane potential at which $h_\infty = 0.5$ and k_h is the steepness coefficient. For the observed individual values, a nonlinear least-squares analysis yielded $V_h = -58 \pm 1$ mV and $k_h = -9 \pm 1$ mV (best fit ± SEE of 12 experiments).

Voltage Dependence of Ca^{2+} Currents

In addition to Na^+ currents, α_2 cells also have voltage-activated Ca^{2+} currents. These were separated from the Na^+ currents by the addition of TTX or the

omission of extracellular Na^+. Fig. 8, *A* and *B*, shows a family of voltage-clamp currents recorded when depolarizing pulses were applied from a holding potential of −70 mV. The currents were maximal within 5 ms and, particularly at negative membrane potentials, showed a tendency toward inactivation. Fig. 8*C* shows the *I-V* relationships for the inward currents recorded in the presence of normal (2.6 mM) and elevated (10.2 mM) concentrations of Ca^{2+}. The fourfold increase of the Ca^{2+} concentration resulted in an 86% increase of the peak Ca^{2+} current. Whereas the current peaked at about −10 mV at 2.6 mM Ca^{2+}, the peak was moved 15 mV in the positive direction in the presence of the high Ca^{2+} concentration. This behavior is in keeping with the well-documented ability of extracellular Ca^{2+} to shift channel gating (Frankenhaeuser and Hodgkin, 1957).

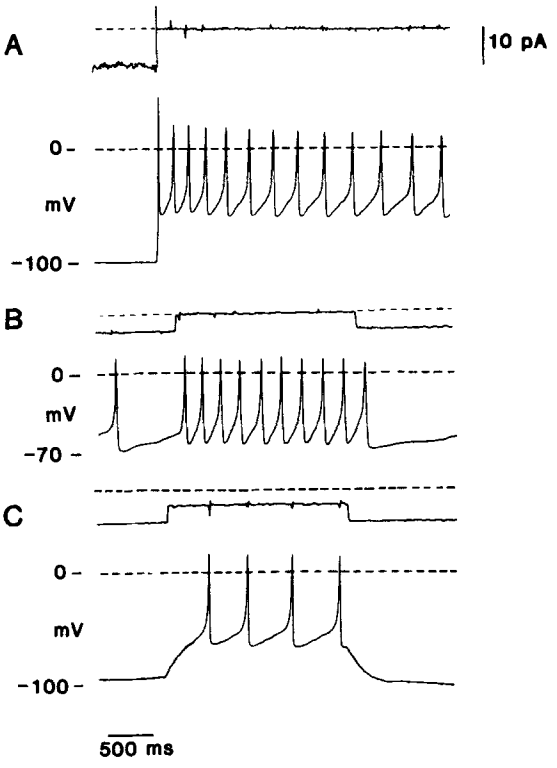

FIGURE 9. Membrane potential recordings from α_2 cells. In each panel, the top trace is the command current and the bottom trace is the membrane potential recording. The dashed lines refer to the zero-current level or zero membrane potential, respectively. (*A*) The cell was initially clamped at −100 mV (holding current, −10 pA). After releasing the clamp, the cell started to produce overshooting action potentials. (*B*) Hyperpolarization to −70 mV (holding current, −5 pA). The cell produced action potentials with a frequency lower than that under unclamped conditions. Injection of 5 pA current (2 s) increased the spike frequency without a change in the interspike membrane potential. (*C*) Hyperpolarization to about −100 mV (holding current, −10 pA) with application of a 5-pA pulse (same current step size as in *B*) resulted in a "burst" of spiking activity superimposed on a "slow wave." All records are from the same cell. The pipettes were filled with intracellular medium E and the bath contained extracellular medium A.

Membrane Potential Recordings from α_2 Cells

Fig. 9*A* shows the membrane potential changes obtained after release of the voltage clamp in a cell initially held at −100 mV. As can be seen, the α_2 cell starts producing regenerative and overshooting (going to 20 mV) action poten-

tials. The frequency was highest immediately after release of the clamp but later stabilized at a lower value. The cell was then hyperpolarized slightly by injection of current (Fig. 9*B*). This reduced the spike frequency but did not affect the interspike membrane potential much. Subsequent injection of a small depolarizing current (~5 pA) produced a train of action potentials. A more marked depolarization was obtained upon current injection when the cell was first hyperpolarized (Fig. 9*C*). Under the latter condition, the membrane potential

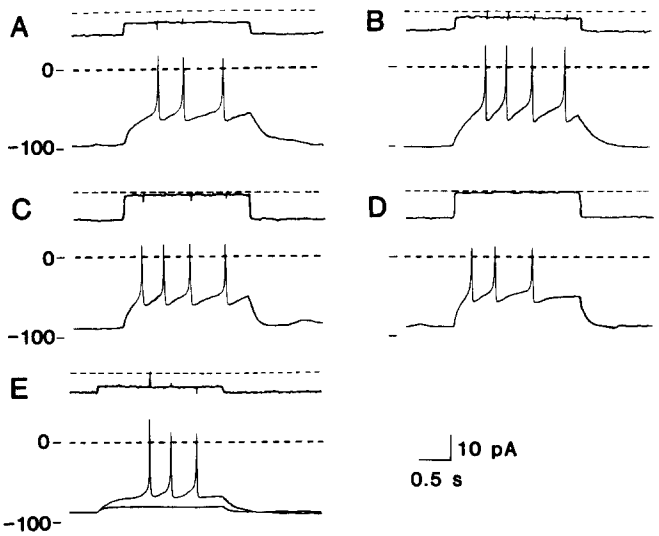

FIGURE 10. Analyses of ionic conductances underlying membrane potential fluctuations using cells hyperpolarized to −100 mV (holding current, −7 to −11 pA). In each panel, the top trace is the command current and the bottom trace is the membrane potential recording. The dashed lines refer to the zero-current level or zero membrane potential, respectively. (*A* and *B*) Raising extracellular Ca^{2+} from 2.6 mM (*A*) to 10.2 mM (*B*) resulted in an increase of spike height. The same cell was used in records *A* and *B*. (*C* and *D*) Records from another cell under control conditions (*C*) and after omission of extracellular Na^{+} (*D*). Note the reduction of spike height. (*E*) Action potentials recorded from a new cell under control conditions (upper trace) and after removing extracellular Ca^{2+} (lower trace). The current traces for control and test conditions exactly superimpose, which indicates that no change in the input resistance of the cell has taken place. Note the abolition of action potentials as well as the reduction of "slow wave" height. The pipettes were filled with medium E and the cells were initially immersed in normal extracellular medium A. Pulses (2 s) were applied at a rate of 0.12 Hz.

of the cell was too negative for action potentials to appear. Injection of the same amount of current as in Fig. 9*B* then produced a slow depolarization from −100 to −60 mV, from which overshooting action potentials were elicited (Fig. 9*C*). A large part of the slow depolarization can undoubtedly be attributed to passive membrane properties. This is suggested by the fact that the time constants for the turn-on and turn-off are about the same. However, as will become clear in Fig. 10*E*, this is not the sole explanation.

Ionic Dependence of Membrane Potential Changes

Figs. 10 and 11 address the question of how the ionic conductances described in this study contribute to the electrical activity shown in Fig. 9. Raising the extracellular Ca^{2+} concentration from 2.6 to 10.2 mM increased the spike height (V_{peak}) by ~10 mV (Figs. 10, *A* and *B*, and 11*B*). Abolition of the Na^+ current (removal of extracellular Na^+) reduced the spike height by ~10 mV, but regenerative action potentials could still be elicited (Figs. 10, *C* and *D*, and 11*A*). In contrast, suppression of the smaller Ca^{2+} current (replacement of extracellular Ca^{2+} with Co^{2+}) while maintaining a normal extracellular Na^+ concentration had more dramatic effects, and action potentials were no longer produced. Under the latter condition, there was also some reduction of the "initial depolarization" obtained when a depolarizing stimulus was applied (Fig. 10*E*). The latter effect was particularly pronounced when a cell with high input resistance was used, but it was generally less obvious than illustrated here. The changes induced when

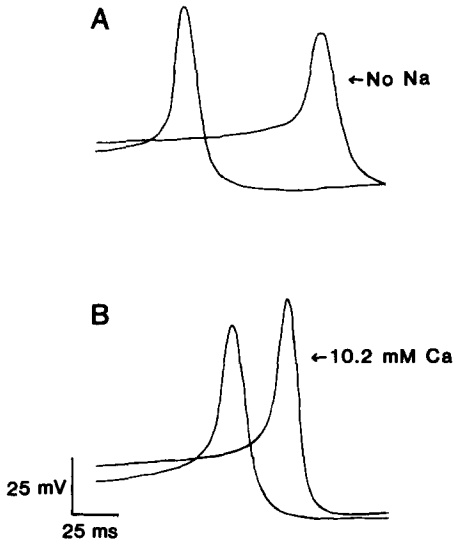

FIGURE 11. Expanded records of traces in Fig. 10. (*A*) Appearance of action potential under control conditions (left) and after removal of Na^+ (right). (*B*) Action potentials recorded under control conditions (left) and after increasing extracellular Ca^{2+} from 2.6 to 10.2 mM (right).

the composition of the extracellular medium was varied are illustrated at greater resolution in Fig. 11. Removal of Na^+ resulted in both a reduction of the spike height and a retardation of the rising phase of the action potential from 9 to 5 V/s (Fig. 11*A*). An increase of extracellular Ca^{2+} from 2.6 to 10.2 mM led to an increase of dV/dt from 9 to 12 V/s (Fig. 11*B*). The observations in Figs. 10 and 11 indicate that the Na^+ and Ca^{2+} currents described in this study contribute to the actual spike. In addition, there is evidence for a second Ca^{2+} conductance activating at potentials close to the threshold of action potential initiation.

DISCUSSION

The introduction of the patch-clamp technique has made possible electrophysiological measurements in cells hitherto inaccessible to such studies. This applies

especially to endocrine organs consisting of different types of cells, as exemplified by the islets of Langerhans. Although it has been possible to characterize extensively the insulin-producing β cells using conventional intracellular electrodes (Henquin and Meissner, 1984), our knowledge about the electrophysiology of the somatostatin-secreting α_1 and glucagon-secreting α_2 cells, which together compose 20–25% of the total cell number, is scanty. Previous work has disclosed that α_2 cells are electrically coupled to β cells (Orci et al., 1976; Michaels and Sheridan, 1981; Meda et al., 1982) and are capable of generating Ca^{2+}-dependent action potentials (Ikeuchi and Yagi, 1982). In the present study, we used the guinea pig as a source of α_2 cells. After injection with the β cell cytotoxic compound streptozotocin, guinea pigs have previously been used as a source of pancreatic islets rich in α_2 cells for studying the mechanisms of glucagon secretion (Petersson et al., 1970). Studies on the ^{45}Ca uptake with such a preparation have suggested that glucose has different effects on the metabolism of Ca^{2+} in pancreatic β and α_2 cells (Berggren et al., 1979).

Employing the whole-cell mode of the patch-clamp technique, we have measured the voltage-activated currents underlying the α_2 cell action potential. The whole-cell mode of the patch-clamp technique involves the replacement of the normal intracellular compartment by the medium in the pipette. Consequently, cytoplasmic factors, which might influence the ionic conductances, will be extensively diluted or even washed out. It was therefore surprising that even during protracted experiments, no major basal conductance developed. The absence of such a resting conductance might explain why α_2 cells produced action potentials at a relatively high rate in the absence of any stimulus. Previous studies on β cells have revealed the existence of a K^+ conductance regulated by intracellular ATP (Cook and Hales, 1984; Findlay et al., 1985; Rorsman and Trube, 1985). No such mode of K^+ outflow could be detected in α_2 cells. Since the insulin-releasing sulfonylureas have been shown to interact specifically with the ATP-regulated K^+ channel (Trube et al., 1986), it is not surprising that most studies have failed to demonstrate an influence of these compounds on the release of glucagon (Luyckx, 1983). In fact, reported actions of tolbutamide on α_2 cells (see review by Luyckx, 1983) may well be secondary to sulfonylurea-stimulated release of insulin and/or somatostatin.

As discussed above, α_2 cells already produce spontaneous action potentials under basal conditions. The frequency of these potentials could be modulated by small variations of the membrane potential, so that a small depolarization markedly increased the number of spikes (see Figs. 3, *C–E*, and 9, *A* and *B*). The significance of this observation is illustrated by the pronounced stimulatory action of arginine on the spike frequency. The action of arginine was characterized by a rapid onset and reversibility. It is thus likely that this positively charged amino acid depolarizes the α_2 cell by electrogenic entry, and not by its metabolic degradation within the cell. Since the voltage-clamp and membrane potential recordings revealed that these action potentials are, at least in part, produced by an inward Ca^{2+} current, it is tempting to conclude that glucagon secretion depends on a stimulated influx of Ca^{2+} into α_2 cells. The notion that an increase of intracellular Ca^{2+} initiates the secretory process in the α_2 cell is further supported by reports of an enhancement of glucagon secretion in the presence

of a supranormal concentration of K^+ (Epstein et al., 1978), a condition that depolarizes the cell and leads to the opening of the voltage-regulated Ca^{2+} channels.

Exposure to glucose is known to inhibit the release of glucagon (Gerich, 1983). However, there was no inhibitory action of glucose on the electrical activity for up to 30 min. Previous studies have revealed that glucose is equally well taken up and metabolized by the α_2 cell in the presence or absence of insulin (Gorus et al., 1984). It is therefore unlikely that the lack of an obvious action of glucose on the electrical activity reflects the absence of sufficient amounts of insulin. Indeed, direct application of insulin failed to affect the spike frequency either in the presence or absence of glucose. The demonstration that glucose is without effect on the electrical activity of α_2 cells is in accordance with recently reported membrane potential recordings from an identified α_2 cell in an intact islet, which indicated an electrical activity in the presence of 11 mM glucose similar to that observed in β cells (Meda et al., 1986). Therefore, it should be considered whether glucose modulates glucagon secretion by influencing the intracellular handling and/or the outward transport of Ca^{2+} rather than the influx. Under conditions where the entry of Ca^{2+} is restricted, glucose is known to inhibit the release of insulin from β cells by reducing intracellular Ca^{2+} (Hellman and Gylfe, 1986). If a similar mechanism is also operational in α_2 cells, it may explain why glucose can inhibit the release of glucagon. It is worthy of note that the suppressor action on glucagon release (Gerich, 1983) shows a sensitivity to glucose similar to the intracellular sequestration of Ca^{2+} in β cells (Hellman and Gylfe, 1986). In α_2 cells, the secretory and electrical activities are already high under basal conditions, and glucose lacks a means by which it can further increase Ca^{2+} influx. Therefore, the intracellular Ca^{2+}-lowering action of glucose will prevail, resulting in the suppression of glucagon release.

Glucose inhibition of glucagon release is dependent on the metabolism of the sugar. Exposure to metabolic poisons such as dinitrophenol and cyanide results in stimulation of the secretory activity of α_2 cells (Edwards and Taylor, 1970), a phenomenon that might be attributed to dumping of intracellularly bound Ca^{2+} into the cytoplasm. Na^+, as well as Ca^{2+}, contributes to the action potential of the α_2 cell. Glucagon-release studies have suggested that opening of the Na^+ channels by veratridine stimulates secretion by mobilizing intracellular Ca^{2+} stores (Kawazu et al., 1981). The existence of Na^+-Ca^{2+} exchange processes has been demonstrated in many excitable tissues, including the pancreatic islets (Hellman and Gylfe, 1986). It is thus conceivable that under physiological conditions the secretory cascade initiated by Ca^{2+} influx can be amplified by the release of organelle-bound Ca^{2+} induced by Na^+ entering during the action potential.

It can be concluded that both Na^+ and Ca^{2+} currents contribute to the depolarizing phase of the action potentials. With the observation that there is an absolute requirement of extracellular Ca^{2+}, but not of Na^+, for the generation of the action potentials, the question arises whether a low-threshold Ca^{2+} current, similar to that proposed to account for the rhythmic firing of action potentials in neurons (Llinàs and Jahnsen, 1982) has a pacemaking role in pancreatic α_2 cells. This possibility will be explored in the following article (Rorsman, 1988).

We thank Dr. G. Trube (Göttingen) for help in setting up the patch-clamp technique in Uppsala and for reading the manuscript, and Dr. A. Schnell-Landström for performing the immunostaining of the α_2 cells. Our thanks are also due to Drs. L. Grimelius and G. Hacker for making unpublished data available.

Financial support was obtained from the Nordic Insulin Foundation, the Swedish Diabetes Association, the Swedish Council for Planning and Coordination of Research, the Swedish Medical Research Council (12x-562), Knut and Alice Wallenberg's Foundation, Syskonen Svenssons Fond, and Amundsons Fond.

Original version received 24 September 1986 and accepted version received 27 March 1987.

REFERENCES

Ashcroft, F. M., D. E. Harrison, and S. J. H. Ashcroft. 1984. Glucose induces closure of single potassium channels in isolated rat pancreatic β-cells. *Nature.* 312:446–448.

Berggren, P.-O., C. G. Östenson, B. Petersson, and B. Hellman. 1979. Evidence for divergent glucose effects on calcium metabolism in pancreatic β and α_2-cells. *Endocrinology.* 105:1463–1468.

Bezanilla, F. 1985. A high capacity recording device based on a digital audio processor and a video cassette recorder. *Biophysical Journal.* 47:437–441.

Brolin, S. E., G. Lundquist, and B. Petersson. 1966. Isolation of A_2-cells from pancreatic islets for ultramicrochemical analyses. *Acta Endocrinologica.* 53:303–309.

Byerly, L., and B. Yazejian. 1986. Intracellular factors for the maintenance of calcium currents in perfused neurones from the snail, *Lymnea stagnalis. Journal of Physiology.* 370:634–650.

Cook, D. L., and N. Hales. 1984. Intracellular ATP directly blocks K^+ channels in pancreatic B-cells. *Nature.* 311:271–273.

Edwards, J. C., and K. W. Taylor. 1970. Fatty acids and the release of glucagon from isolated guinea pig islets of Langerhans incubated in vitro. *Biochimica et Biophysica Acta.* 215:310–315.

Epstein, G., R. Fanska, and G. M. Grodsky. 1978. The effects of potassium and valinomycin on insulin and glucagon secretion in perfused rat pancreas. *Endocrinology.* 103:2207–2215.

Fedulova, S. A., P. G. Kostyuk, and N. S. Veselovsky. 1985. Two types of calcium channels in the somatic membrane of new-born rat dorsal root ganglion neurones. *Journal of Physiology.* 359:431–446.

Fenwick, E. M., A. Marty, and E. Neher. 1982*a*. A patch-clamp study of bovine chromaffin cells and their sensitivity to acetylcholine. *Journal of Physiology.* 331:557–597.

Fenwick, E. M., A. Marty, and E. Neher. 1982*b*. Sodium and calcium channels in bovine chromaffin cells. *Journal of Physiology.* 331:599–635.

Findlay, I., M. J. Dunne, and O. H. Petersen. 1985. ATP-sensitive inward rectifier and voltage- and calcium-activated K^+ channels in cultured pancreatic islet cells. *Journal of Membrane Biology.* 88:165–172.

Fischmeister, R., R. K. Ayer, Jr., and R. L. De Haan. 1986. Some limitations of the cell-attached patch clamp technique: a two-electrode analysis. *Pflügers Archiv.* 406:73–82.

Frankenhaeuser, B., and A. L. Hodgkin. 1957. The action of calcium on the electrical properties of squid axons. *Journal of Physiology.* 137:218–244.

Gerich, J. E. 1983. Glucose in the control of glucagon secretion. *In* Handbook of Experimental Pharmacology. P. J. Lefebvre, editor. Springer-Verlag, Berlin. 66/II:3–18.

Gorus, F. K., W. J. Malaisse, and D. G. Pipeleers. 1984. Differences in glucose handling by pancreatic A- and B-cells. *Journal of Biological Chemistry.* 259:1196–1200.

Hamill, O. P., A. Marty, E. Neher, B. Sakmann, and F. J. Sigworth. 1981. Improved patch-clamp techniques for high-resolution current recording from cells and cell-free membrane patches. *Pflügers Archiv.* 391:85–100.

Hellman, B., and E. Gylfe. 1986. Calcium and the control of insulin secretion. *In* Calcium and Cell Function. W. Y. Cheung, editor. Academic Press, Inc., Orlando, FL. VI:253–326.

Henquin, J. C., and H. P. Meissner. 1984. Significance of ionic fluxes and changes in membrane potential for stimulus-secretion coupling in pancreatic B-cells. *Experientia.* 40:1043–1052.

Hille, B. 1984. Ionic Channels of Excitable Membranes. Sinauer Associates, Inc., Sunderland, MA. 58–75.

Hodgkin, A. L., and A. F. Huxley. 1952*a*. Currents carried by sodium and potassium ions through the membrane of the giant axon of *Loligo*. *Journal of Physiology.* 116:449–472.

Hodgkin, A. L., and A. F. Huxley. 1952*b*. The dual effect of membrane potential on sodium conductance in the giant squid axon of *Loligo*. *Journal of Physiology.* 116:497–506.

Ikeuchi, M., and K. Yagi. 1982. Pancreatic A cell generates action potential. *Japanese Journal of Physiology.* 32:873–878.

Kawazu, S., M. Ikeuchi, M. Kikuchi, M. Kanazawa, W. Y. Fujimoto, and K. Kosaka. 1981. Dual effects of veratridine on glucagon and insulin secretion. Dependence upon extracellular and intracellular calcium. *Diabetes.* 30:446–450.

Leclerq-Meyer, V., and W. J. Malaisse. 1983. Ions in the control of glucagon release. *In* Handbook of Experimental Pharmacology. P. J. Lefèbvre, editor. Springer-Verlag, Berlin. 66/II:59–74.

Lernmark, Å. 1974. The preparation of, and studies on, free cell suspensions from mouse pancreatic islets. *Diabetologia.* 10:431–438.

Llinàs, R., and H. Jahnsen. 1982. Electrophysiology of mammalian thalamic neurones *in vitro*. *Nature.* 297:406–408.

Lundquist, G., S. E. Brolin, R. H. Unger, and A. M. Eisentraut. 1970. The cellular origin of pancreatic glucagon. *In* The Structure and Metabolism of the Pancreatic Islets. S. Falkmer, B. Hellman, and I.-B. Täljedal, editors. Pergamon Press, Oxford. 115–121.

Luyckx, A. S. 1983. Pharmacologic compounds affecting glucagon secretion. *In* Handbook of Experimental Pharmacology. P. J. Lefèbvre, editor. Springer-Verlag, Berlin. 66/II:175–201.

Martell, A. E., and R. M. Smith. 1974. Critical Stability Constants. Vol. I: Amino Acids. 469 pp. Vol. II: Amines. 415 pp. Plenum Publishing Corp., New York, NY.

Meda, P., E. Kohen, C. Kohen, A. Rabinovitch, and L. Orci. 1982. Direct communication of homologous and heterologous endocrine islet cells in culture. *Journal of Cell Biology.* 92:221–226.

Meda, P., R. M. Santos, and I. Atwater. 1986. Direct identification of electrophysiologically monitored cells within intact mouse islets of Langerhans. *Diabetes.* 35:232–236.

Meissner, H. P., J. C. Henquin, and M. Preissler. 1978. Potassium dependence of the membrane potential of pancreatic β-cells. *FEBS Letters.* 94:87–89.

Michaels, R. L., and J. D. Sheridan. 1981. Islet of Langerhans dye coupling among immunocytochemically distinct cell types. *Science.* 214:801–803.

Orci, L., F. Malaisse-Lagae, M. Ravazzola, D. Rouiller, A. E. Renold, A. Perrelet, and R. H. Unger. 1976. A morphological basis for intracellular communication between α- and β-cells in the endocrine pancreas. *Journal of Clinical Investigation.* 56:1066–1070.

Petersson, B. 1966. Isolation and characterization of different types of pancreatic islet cells in guinea pigs. *Acta Endocrinologica.* 53:480–488.

Petersson, B., C. Hellerström, and R. Gunnarsson. 1970. Structure and metabolism of the

pancreatic islets in streptozotocin-treated guinea pigs. *Hormone and Metabolic Research.* 2:313–317.

Petersson, B., C. Hellerström, and B. Hellman. 1962. Some characteristics of the two types of A-cells in the islets of Langerhans of guinea pigs. *Zeitschrift für Zellforschung.* 57:559–566.

Pipeleers, D. G., P. A. In't Veld, M. Van De Winkel, E. Maes, F. C. Schuit, and W. Gepts. 1985. A new *in vitro* model for the study of pancreatic A and B cells. *Endocrinology.* 117:806–816.

Rorsman, P. 1986. Patch-clamp studies on pancreatic glucagon- and insulin-secreting cells. *Acta Universitas Upsaliensis.* 70:1–34.

Rorsman, P. 1988. Two types of Ca^{2+} currents with different sensitivities to organic Ca^{2+} channel antagonists in guinea pig pancreatic α_2 cells. *Journal of General Physiology.* 91:243–254.

Rorsman, P., P. Arkhammar, and P.-O. Berggren. 1986. Voltage-activated Na^+ currents and their suppression by phorbol ester in clonal insulin-producing RINm5F-cells. *American Journal of Physiology.* 251:912–919.

Rorsman, P., and G. Trube. 1985. Glucose dependent K^+ channels in pancreatic β-cells are regulated by intracellular ATP. *Pflügers Archiv.* 405:305–309.

Rorsman, P., and G. Trube. 1986. Calcium and delayed potassium currents in mouse pancreatic β-cells under voltage-clamp conditions. *Journal of Physiology.* 374:531–550.

Satin, L. S., and D. L. Cook. 1986. Voltage-gated inward currents in pancreatic islet B-cells. *Biophysical Journal.* 49:199*a*. (Abstr.)

Trube, G., P. Rorsman, and T. Ohno-Shosaku. 1986. Opposite effects of tolbutamide and diazoxide on the ATP-dependent K^+ channel in mouse pancreatic β-cells. *Pflügers Archiv.* 407:493–499.

Wesslén, N., D. Pipeleers, M. Van De Winkel, P. Rorsman, and B. Hellman. 1987. Glucose stimulates the entry of Ca^{2+} into the insulin-producing β cells but not into the glucagon-producing α_2 cells. *Acta Physiologica Scandinavica.* 131:230–234.